

Enhanced NMR with Optical Pumping Yields ^{75}As Signals Selectively from a Buried GaAs Interface

Matthew M. Willmering,[†] Zayd L. Ma,[†] Melanie A. Jenkins,[‡] John F. Conley, Jr.,[‡] and Sophia E. Hayes^{*,†} 

[†]Department of Chemistry, Washington University, Saint Louis, Missouri 63130, United States

[‡]School of Electrical Engineering and Computer Science, Oregon State University, Corvallis, Oregon 97331, United States

Supporting Information

ABSTRACT: We have measured the ^{75}As signals arising from the interface region of single-crystal semi-insulating GaAs that has been coated and passivated with an aluminum oxide film deposited by atomic layer deposition (ALD) with optically pumped NMR (OPNMR). Using wavelength-selective optical pumping, the laser restricts the volume from which OPNMR signals are collected. Here, OPNMR signals were obtained from the interface region and distinguished from signals arising from the bulk. The interface region is highlighted by interactions that disrupt the cubic symmetry of the GaAs lattice, resulting in quadrupolar satellites for nuclear $I = \frac{3}{2}$ isotopes, whereas NMR of the “bulk” lattice is nominally unsplit. Quadrupolar splitting at the interface arises from strain based on lattice mismatch between the GaAs and ALD-deposited aluminum oxide due to their different coefficients of thermal expansion. Such spectroscopic evidence of strain can be useful for measuring lattice distortions at heterojunction boundaries and interfaces.

Semiconductor heterojunctions are created in solid-state electronic devices when two materials with dissimilar band gap energies are chemically bonded to one another.¹ For higher-performing electronic devices to be created, a better understanding of the interface at the heterojunction is necessary. The heterojunction studied here ($\text{Al}_2\text{O}_3/\text{GaAs}$) has been proposed for metal-oxide semiconductor field-effect transistors (MOSFETs),^{2,3} MOS capacitors,³ and as a passivation layer for GaAs.^{2–5} By determining the interfacial structure in heterojunctions, manipulation of growth and synthetic procedures can be followed for their effect on the electronic performance of devices.

Solid-state nuclear magnetic resonance (NMR) has been used to study inorganic semiconductors;⁶ however, conventional NMR techniques are usually incapable of measuring spectra from interfaces due to the limit of $\sim 10^{16}$ spins for detection. Hyperpolarization⁷ allows a lower detection threshold for NMR spectroscopy of such samples.

Optical pumping in direct gap semiconductors uses laser excitation to form polarized conduction electrons. By using circularly polarized light, optical absorption selection rules create nonequilibrium electron spin populations within the conduction band that are subsequently captured at defect sites. Hyperfine interactions between captured electrons and

proximate nuclei result in the transfer of electron spin polarization to the nuclei. Optically pumped NMR (OPNMR)^{8,9} detects the nuclear magnetization with traditional radio frequency NMR methods. The OPNMR signals are photon energy dependent, and vary as a function of the laser penetration depth because the laser-excited electrons are the origin of the hyperpolarization.¹⁰ Thus, the laser intensity and spatial distribution throughout the sample determines the portion of the sample being detected.

The nuclear isotope studied here is quadrupolar ^{75}As (nuclear spin quantum number, $I = \frac{3}{2}$), which couples to any electric field gradient (EFG) present, resulting in a splitting of the NMR resonance.^{11,12} Stress perturbs structures away from perfect cubic symmetry through bond distortions; thus, lattice strain can be detected from the amount a quadrupolar resonance is split.^{13–15} Strain in GaAs has been studied previously by OPNMR (and optically detected NMR) methods to determine nuclear spin temperatures,¹⁶ bandstructure effects,¹⁷ spatial inhomogeneities of strain,¹⁵ and dominant polarization mechanisms.^{18–20}

A $400\text{ }\mu\text{m}$ bulk semi-insulating single crystal of GaAs (ITME, grown along [100], lot 2137, polished on one side) was used as a substrate. A thin film of amorphous alumina, hereafter denoted Al_2O_3 , was deposited using atomic layer deposition (ALD) on the polished side of the GaAs. The deposition temperature was $300\text{ }^\circ\text{C}$. Four pulses of trimethyl aluminum were used to remove the native oxides on the surface of the GaAs substrate^{4,5} prior to ALD growth. The final thickness of the Al_2O_3 film was 11.2 nm and is shown schematically in Figure S1.

The experimental procedures for OPNMR have been described previously with critical parameters noted:^{9,21} The external magnetic field (B_0) was 4.7 T. B_1 excitation strength was ~ 20 kHz; σ^+ polarization and laser power were held constant at 100 mW. The sample was irradiated for a time period of τ_L (90 s) after the saturation sequence; a short period of time (τ_D) was inserted where the laser was shuttered (~ 1 s), and the NMR spectra were then acquired by a quadrupolar echo²² pulse sequence (using 55° pulses) while the laser was shuttered (Figure S2). Tip angles of 55° were used to observe the asymmetry of the satellites and refocus the dipolar and quadrupolar interactions.^{23–25} The $90^\circ - \tau - 64^\circ$ pulse sequence of refs 23 and 24 results in symmetric satellites that do not

Received: August 26, 2016

Published: March 3, 2017

properly depict the spin temperature. The $55^\circ-\tau-55^\circ$ sequence represents the best (approximate) trade-off between optimal refocusing of the central transition and the satellites for a spin- $\frac{3}{2}$ nucleus.²⁵

The spatial regions where the light is absorbed determine the portion of the sample that can be observed. The size of such regions is governed by the beam diameter, the position of the laser on the sample, and the penetration depth of the light. The size of these regions has been used to previously model the photon energy dependence of OPNMR spectra.¹⁰ In this study, all photon energies used were much smaller than the band gap of the Al_2O_3 (at ~ 9 eV²⁶), allowing the laser to pass through the ALD film to the GaAs substrate underneath. The laser intensity then decays exponentially with depth⁹ into the GaAs. At high optical absorption values, the laser excites conduction electrons in only the interfacial region where strain is present. The minimal penetration depth of the laser is estimated as < 275 nm²⁷ in the OPNMR experiments. At lower photon energies, the laser will penetrate deeper into the sample and observe a large fraction of the bulk (~ 400 μm thick) GaAs crystal away from the interface.

Because of the ALD deposition parameters (i.e., temperature and surface pretreatment), the resulting Al_2O_3 film is amorphous, reducing most of the strain due to the lattice mismatch of the two structures. However, because growth of the ALD film occurs at higher temperatures, thermal strain can develop when the sample cools and the materials compress according to their thermal expansion coefficients. The thermal strain resulting from differing thermal coefficients of the film and substrate is expressed as²⁸

$$\epsilon = (\alpha_{\text{film}} - \alpha_{\text{substrate}})(T_i - T_f) \quad (1)$$

where ϵ is the resulting strain, α is the thermal expansion coefficient, and T is the temperature of the growth initially ($T_i = 573$ K) and the final temperature ($T_f = 6$ K). The difference in thermal expansion coefficients is 1.3×10^{-6} K⁻¹.²⁹ The resulting thermal strain expected for our experiments is 7.37×10^{-4} (dimensionless units), which will be most intense at the interface and dissipate with distance.³⁰ The strain at 6 K will create an electric field gradient (EFG) and results in splitting into a quadrupolar line shape. Deeper into the GaAs bulk crystal, the strain diminishes until the nuclear spin environment is a single unsplit resonance owing to the cubic symmetry (zinc blend crystal structure) of the lattice.

The diminishing amount of strain experienced by the ^{75}As atoms results in a distribution of quadrupolar environments observed by conventional NMR (termed “thermally polarized”) of the Al_2O_3 -coated GaAs wafer at 6 K. A narrow “bulk” crystalline resonance (fwhm ≈ 1.6 kHz) is found but with evident broadening at the baseline (dashed line, Figure 1a). An ^{75}As OPNMR spectrum from an uncoated GaAs wafer (“bare GaAs”, solid line) is also shown, which has no interface strain (optical pumping selects signals from the top region of the sample). The NMR signal is a narrow single-crystal resonance with little broadening at the base. OPNMR enhances the signal, but without the ALD layer, only the crystalline bulk GaAs is observed. Notably in the Al_2O_3 -coated GaAs sample in Figure 1a, the limited number of nuclear spins at the interface are overwhelmed by the large fraction of signal coming from the bulk lattice when detected conventionally. The use of optical pumping overcomes this issue by limiting the signal to layers

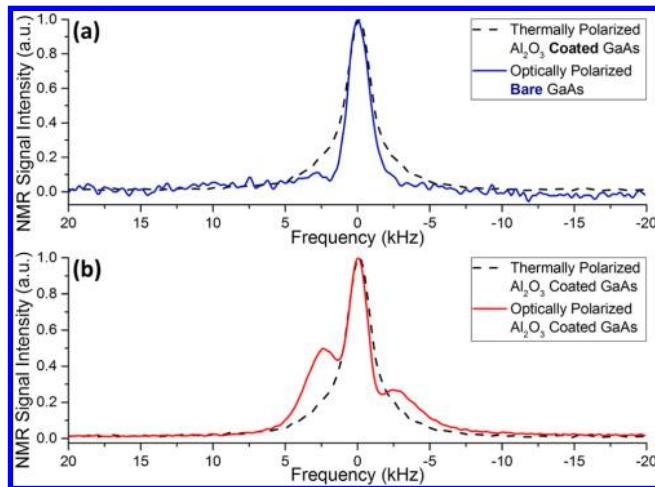


Figure 1. ^{75}As NMR (black dashed line) and OPNMR (blue and red solid lines) of GaAs. (a) Comparison of the conventional spectrum of the coated GaAs (black) to an optically pumped spectrum of “bare” GaAs with its native oxide present (blue). (b) Comparison of the OPNMR (red) and NMR (black) spectra of the Al_2O_3 -coated GaAs. The optically pumped NMR spectra were recorded at a wavelength of 819.3 nm. The spectra have been normalized.

near the top of the sample, capitalizing on the shallow penetration depth of the laser at specific photon energies.

Optically pumped NMR of the Al_2O_3 -coated GaAs sample (shown in red, Figure 1b) using photon energies in excess of the excitonic absorption (~ 1.517 eV) can be compared as well. OPNMR of the Al_2O_3 -coated GaAs produces three peaks; the two outer peaks are the quadrupolar satellites, and the middle peak is predominantly³¹ from the central transition. The satellite intensities are asymmetric, indicating high levels of nuclear polarization,¹⁶ which is evidence of spin cooling below that of the “high temperature approximation”.³² With the large polarization present, larger transition intensities are expected at lower (positive spin temperature) or higher (negative spin temperature) frequencies.

The first order quadrupolar splitting¹² given by

$$\nu_Q = \frac{3eQV_{zz}}{8I(2I-1)h} (3\cos^2\theta - 1) \quad (2)$$

relates the magnitude of the EFG to a splitting. In the equation, eQ is the nuclear electric quadrupole moment, V_{zz} is the largest component of the EFG tensor, and θ is the angle between the EFG and the external magnetic field. The satellite peaks do not fit to perfect Gaussian lineshapes as they have asymmetric “tails” distributed away from the central transition (Figure 2); this spectral feature is attributable to a distribution of EFGs, and therefore ν_Q , arising from the perturbative effects of the interface, detecting different amounts of strain likely as a function of the distance from the top of the sample.

The two asymmetrically shaped quadrupolar satellites are challenging to deconvolute given their lineshapes. Using the central transition resonance in the “bare” GaAs spectrum (fwhm ≈ 1.5 kHz), we can fit this portion and distinguish its area from the two satellites. Using simple numerical integration, their areas can be compared to that of the central transition. Table 1 lists the relative intensities and splittings of the satellites. In the work of Suemitsu and co-workers,²³ radial EFGs for isolated point defects were simulated using a function

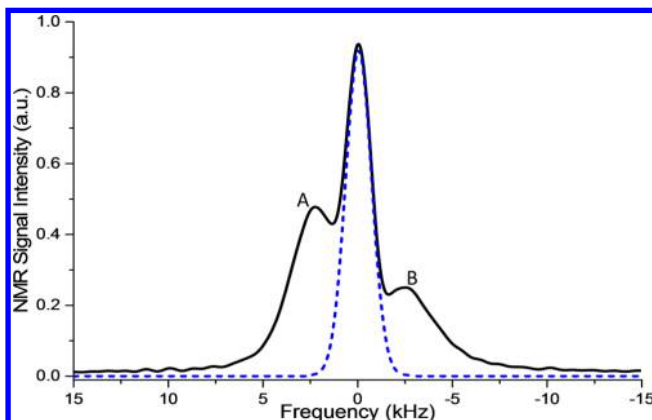


Figure 2. ^{75}As OPNMR of the alumina-coated GaAs showing the central transition using a Gaussian peak with a line width fixed to that of the “bare” ^{75}As OPNMR. The spectrum was recorded using 819.3 nm light.

Table 1. Peak Parameters Acquired by Numerical Integration of Figure 2^a

resonance	relative intensity	contribution to central transition
central transition	10.0	
satellite A	8.12	$\frac{4}{6} \times 8.12 = 5.42$
satellite B	5.94	$\frac{4}{6} \times 5.94 = 3.96$
		$\sum = 9.37 \pm 0.59$

^aThe intensities are relative to that of the central peak intensity set to a value of 10.0.

to model combined dipolar and quadrupolar interactions. This model does not fit our lineshapes.

Because the theoretical peak intensity in a quadrupolar $I = \frac{3}{2}$ spectrum is 3:4:3 using small tip angles,³³ the percent of signal due to the strained nuclei can be calculated. Conservatively, if an estimate is made from the average of the two satellites’ integrated areas,³⁴ $93.7 \pm 5.9\%$ (area = 9.37) of the observed nuclei are strained based on the data in Table 1. We ascribe the small fraction of extra intensity in the central transition to that of unstrained ^{75}As atoms being optically pumped.

It is worth noting that the observed NMR signal decays to the baseline at approximately ± 15 kHz, corresponding to a maximum observed strain of 7.53×10^{-5} .¹⁷ The expected strain (see eq 1) is predicted to be even larger; that no satellites are observed (at larger splittings) suggests that the “missing” intensity could be indicative of either a depletion zone at the interface¹⁸ or too few nuclear spins in the highly strained portions for detection.

The effect of laser penetration depth, governed by the optical absorption coefficient, can be seen from the OPNMR spectra recorded as a function of photon energy in Figure 3. The vertical lines correspond to the (theoretical) wavelengths for the excitonic and band gap transition energies at 0 K.³⁵ Because our experiments were performed at 6 K, the precise photon energies for the transitions should be slightly shifted to a higher wavelength (lower energy). The spectrum at 821.3 nm (below E_g , the band gap energy) shows a line shape dominated by the central peak, which masks the satellite peaks due to the deeper penetration of the laser (to tens or hundreds of micrometers). We do observe broadening at the base similar to that seen by conventional NMR. The spectrum pumped at 818.3 nm is

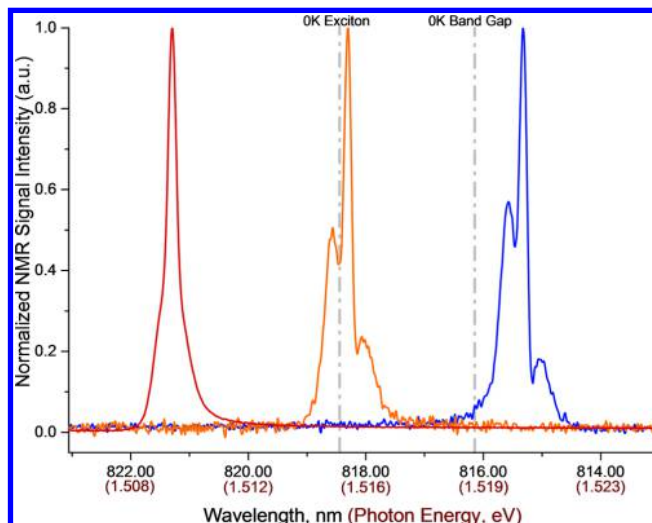


Figure 3. Intensity-normalized ^{75}As OPNMR spectra at various photon energies/wavelengths. The spectra (from left to right) are in order of decreasing wavelength (increasing photon energy) with the central transition positioned over the corresponding optical excitation wavelength. Theoretical positions of the band gap and exciton absorption energies are shown as dashed lines.

polarized by laser excitation of a bound exciton,³⁶ which results in a very shallow penetration depth because of the intense absorption at this wavelength.¹⁰ Notably, it is at this photon energy (wavelength) where the quadrupolar satellites are clearly resolved. For the spectrum with an optical pumping wavelength of 815.3 nm, the polarization remains relatively the same. Because of the large increase in the absorption coefficient at and above the band gap energy, all of the spectra above the band gap originate from areas of strain, whereas the spectra below the band gap cannot be deconvoluted due to the large contribution of the unstrained GaAs.

Other recent studies in OPNMR of strained GaAs have shown evidence of quadrupolar splitting, reporting a significant dependence on laser power.^{18–20} Their studies used sub-bandgap irradiation, revealing both a positive spin temperature at low laser power (ascribed to quadrupolar relaxation close to defect sites) and a resolved quadrupolar splitting attributed to strain throughout the sample exhibited only with high laser power arising from hyperfine relaxation (and negative spin temperature) for σ^+ light. With high laser power and sub-bandgap irradiation, a line shape dominated by the central transition is observed here. Our work has strain concentrated at the near surface accessed by high photon energy whereas others have strain throughout.

In conclusion, NMR spectra of the GaAs interface region was obtained by optical pumping. The thin film Al_2O_3 on the GaAs strains the underlying interface resulting in quadrupolar splitting at cryogenic temperatures. Optical pumping was required to observe this smaller number of spins by NMR. Surface/interface enhancement allowed the quadrupolar split signals of the near-interface As atoms to be discriminated; such spectroscopy gives promise for characterization of interface structures by OPNMR methods.

ASSOCIATED CONTENT

Supporting Information

The Supporting Information is available free of charge on the ACS Publications website at DOI: [10.1021/jacs.6b08970](https://doi.org/10.1021/jacs.6b08970).

OPNMR experimental setup, pulse sequence used for acquisition of the data, and error calculations (PDF)

AUTHOR INFORMATION

Corresponding Author

*hayes@wustl.edu

ORCID

Sophia E. Hayes: 0000-0002-2809-6193

Notes

The authors declare no competing financial interest.

ACKNOWLEDGMENTS

This work was supported by the National Science Foundation through Grants DMR-1206447 and CHE-1606982.

REFERENCES

- (1) Franciosi, A.; Van de Walle, C. G. *Surf. Sci. Rep.* **1996**, *25*, 1–140.
- (2) Huang, M. L.; Chang, Y. C.; Chang, C. H.; Lee, Y. J.; Chang, P.; Kwo, J.; Wu, T. B.; Hong, M. *Appl. Phys. Lett.* **2005**, *87*, 1–3.
- (3) Dalapati, G. *IEEE Trans. Electron Devices* **2007**, *54*, 1831–1837.
- (4) Hinkle, C. L.; Sonnet, A. M.; Vogel, E. M.; McDonnell, S.; Hughes, G. J.; Milojevic, M.; Lee, B.; Aguirre-Tostado, F. S.; Choi, K. J.; Kim, H. C.; Kim, J.; Wallace, R. M. *Appl. Phys. Lett.* **2008**, *92*, 071901.
- (5) Lee, H. D.; Feng, T.; Yu, L.; Mastrogiovanni, D.; Wan, A.; Gustafsson, T.; Garfunkel, E. *Appl. Phys. Lett.* **2009**, *94*, 10–13.
- (6) Yesinowski, J. P. *Top. Curr. Chem.* **2011**, *306*, 229–312.
- (7) Reimer, J. A. *Solid State Nucl. Magn. Reson.* **2010**, *37*, 3–12.
- (8) Tycko, R.; Barrett, S. *eMagRes* **2001**, *1*, 711–719.
- (9) Hayes, S. E.; Mui, S.; Ramaswamy, K. *J. Chem. Phys.* **2008**, *128*, 052203.
- (10) Mui, S.; Ramaswamy, K.; Hayes, S. E. *Phys. Rev. B: Condens. Matter Mater. Phys.* **2007**, *75*, 1–8.
- (11) Freude, D. Nuclear magnetic resonance and electron spin resonance spectroscopy. In *Encyclopedia of Analytical Chemistry*; Meyers, R., Ed.; John Wiley & Sons, Ltd: Chichester, UK, 2000; Chapter Quadrupolar Nuclei in Solid-State Nuclear Magnetic Resonance, pp 12188–12224.
- (12) Ashbrook, S. E. *Phys. Chem. Chem. Phys.* **2009**, *11*, 6892–6905.
- (13) Guerrier, D. J.; Harley, R. T. *Appl. Phys. Lett.* **1997**, *70*, 1739.
- (14) Zwanziger, J. W.; Werner-Zwanziger, U.; Shaw, J. L.; So, C. *Solid State Nucl. Magn. Reson.* **2006**, *29*, 113–118.
- (15) Eickhoff, M.; Lenzmann, B.; Suter, D.; Hayes, S. E.; Wieck, A. D. *Phys. Rev. B: Condens. Matter Mater. Phys.* **2003**, *67*, 085308.
- (16) Paravastu, A.; Reimer, J. *Phys. Rev. B: Condens. Matter Mater. Phys.* **2005**, *71*, 045215.
- (17) Wood, R. M.; Saha, D.; McCarthy, L. A.; Tokarski, J. T.; Sanders, G. D.; Kuhns, P. L.; McGill, S. A.; Reyes, A. P.; Reno, J. L.; Stanton, C. J.; Bowers, C. R. *Phys. Rev. B: Condens. Matter Mater. Phys.* **2014**, *90*, 155317.
- (18) King, J. P.; Li, Y.; Meriles, C. a.; Reimer, J. a. *Nat. Commun.* **2012**, *3*, 918.
- (19) Li, Y.; King, J. P.; Peng, L.; Tamargo, M. C.; Reimer, J. A.; Meriles, C. A. *Appl. Phys. Lett.* **2011**, *98*, 1–4.
- (20) Li, Y.; King, J. P.; Reimer, J. A.; Meriles, C. A. *Phys. Rev. B: Condens. Matter Mater. Phys.* **2013**, *88*, 235211.
- (21) Sesti, E. L.; Worthoff, W.; Wheeler, D. D.; Suter, D.; Hayes, S. E. *J. Magn. Reson.* **2014**, *246*, 130–135.
- (22) Larsen, F. H.; Jakobsen, H. J.; Ellis, P. D.; Nielsen, N. C. *J. Phys. Chem. A* **1997**, *101*, 8597–8606.
- (23) Suemitsu, M.; Nakajo, N. *J. Appl. Phys.* **1989**, *66*, 3178–3186.
- (24) Suemitsu, M.; Nishijima, M.; Miyamoto, N. *Appl. Phys. Lett.* **1990**, *57*, 398.
- (25) Butterworth, J. *Proc. Phys. Soc., London* **1965**, *86*, 297.
- (26) Ye, P. D.; Wilk, G. D.; Kwo, J.; Yang, B.; Gossmann, H. J. L.; Frei, M.; Chu, S. N. G.; Mannaerts, J. P.; Sergent, M.; Hong, M.; Ng, K. K.; Bude, J. *IEEE Electron Device Lett.* **2003**, *24*, 209–211.
- (27) Vasilenko, D. V.; Luk'yanova, N. V.; Seisyan, R. P. *Semiconductors* **1999**, *33*, 15–19.
- (28) Huang, J.; Ye, Z.; Lu, H.; Que, D. *J. Appl. Phys.* **1998**, *83*, 171–173.
- (29) Chakraborti, D. Ph.D. Thesis, North Carolina State University, Raleigh, NC, 2007.
- (30) Detchprohm, T.; Hiramatsu, K.; Itoh, K.; Akasaki, I. *Jpn. J. Appl. Phys.* **1992**, *31*, 1454–1456.
- (31) The central peak would be the combination of the central transition of the quadrupolar split spectrum and signal from any unsplit bulk GaAs.
- (32) Goldman, M. *Encycl. NMR* **2012**, *5*, 2437–2446.
- (33) Man, P. P.; Klinowski, J.; Trokiner, A.; Zanni, H.; Papon, P. *Chem. Phys. Lett.* **1988**, *151*, 143–150.
- (34) de Boer, W.; Borghini, M.; Morimoto, K.; Niinikoski, T. O.; Udo, F. *J. Low Temp. Phys.* **1974**, *15*, 249–267.
- (35) Madelung, O. *Semiconductors – Basic Data*, 2nd ed.; Springer-Verlag: Berlin, 1996; p 317.
- (36) Lew Yan Voon, L.; Willatzen, M. *The k.p Method: Electronic Properties of Semiconductors*; Springer-Verlag: Berlin Heidelberg, 2009.